Table of Contents

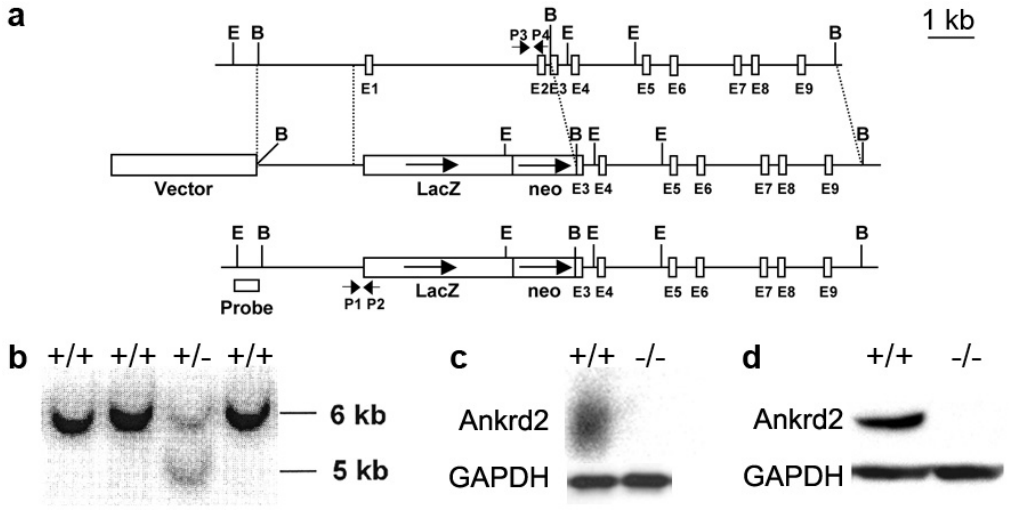

Figure S1. Targeting of the *Ankrd2* gene. Targeting strategy for generation of Ankrd2 KO mice. (a) A restriction map of the relevant genomic region of Ankrd2 is shown on the top, the targeting construct is shown in the center, and the mutated locus after recombination is shown on the bottom. B, BamHI; E, EcoRI; neo, neomycin resistance gene; E, Exon. (b) Detection of WT and targeted alleles by Southern blot analysis after digestion with EcoRI using the probe indicated in A. (c) Northern blot analysis for detection of Ankrd2 RNA. Aliquots of 10 μg of total RNA isolated from skeletal muscle of WT and Ankrd2 KO mice were analyzed using a cDNA probe spanning the entire coding region of Ankrd2. A GAPDH probe was used as a loading control. (d) Western blot analysis on skeletal muscle lysate from WT and Ankrd2 KO mice using anti-Ankrd2 antibodies (Miller et al., 2003). GAPDH was used as a loading control.

a

Sample comparison	Stage 1		Stage 2		Stage 3	
	logFC	SD	logFC	SD	logFC	SD
Ankrd2-WT vs GFP-WT	2.55	0.23	2.87	0.27	3.07	0.18
Ankrd2-KO vs GFP-WT	1.98	0.1	1.54	0.53	1.9	0.38

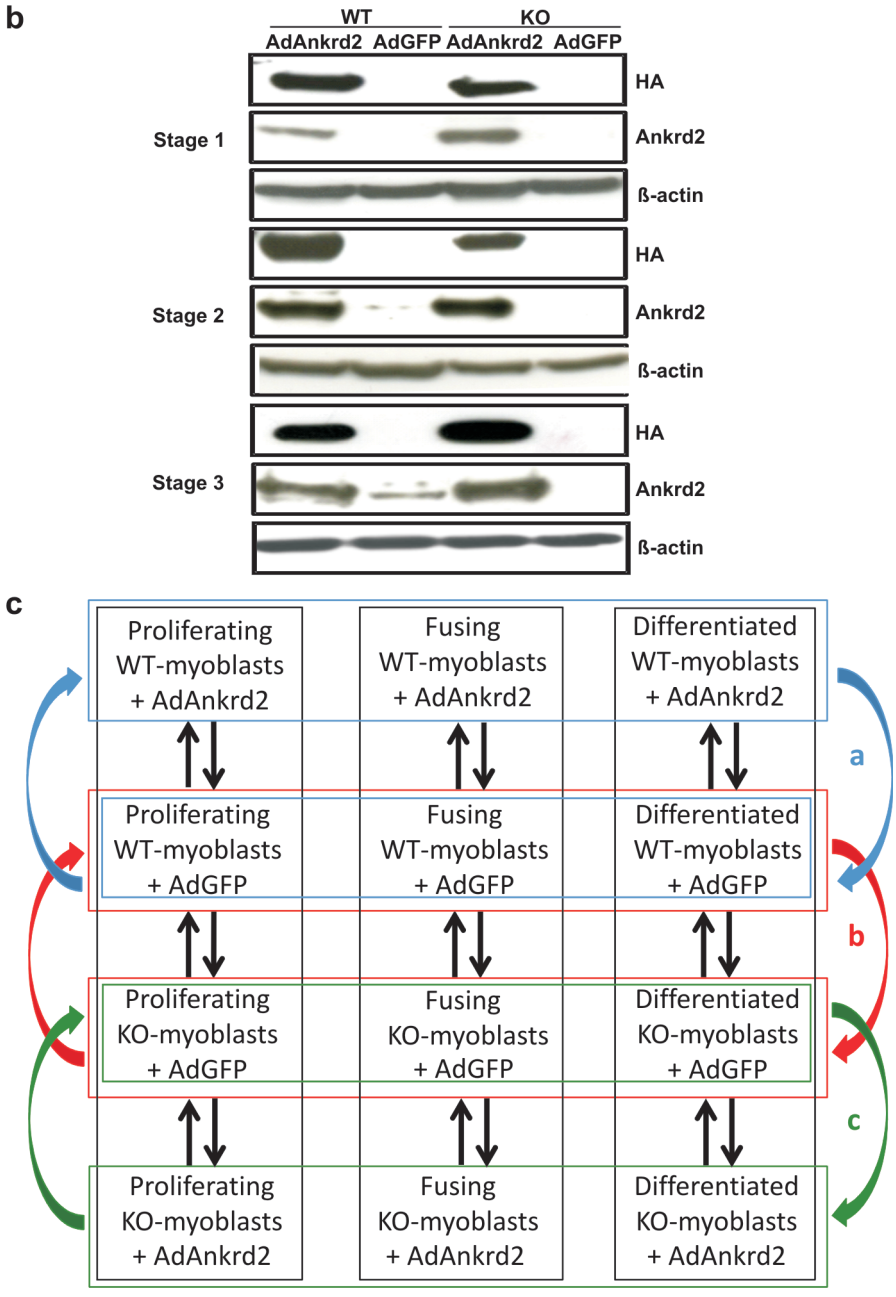

Figure S2. Gene expression analyses on AdAnkrd2 and AdGFP-infected primary myoblasts and quantification of Ankrd2 mRNA and protein levels. (a) Relative quantification of Ankrd2 mRNA levels in proliferating (stage 1), fusing (stage 2) and differentiated (stage 3) WT and Ankrd2 KO myoblasts infected with AdAnkrd2 or AdGFP as determined by qRT-PCR analysis (n = 3). Standard deviations (SD) were estimated using the error propagation theory. LogFC, fold change of logarithmic values. (b) Representative Western blots showing Ankrd2 levels in AdAnkrd2-infected proliferating and differentiating myoblasts as determined using anti-Ankrd2 and anti-HA-tag antibodies. (c) Schematic summary of comparisons between gene signatures obtained from proliferating, fusing, and differentiated WT and Ankrd2 KO primary myoblasts infected with AdAnkrd2 or AdGFP.

Table S1. KEGG pathway enrichment analysis for up- and down-regulated genes in AdAnkrd2- compared to control AdGFP-infected WT cells at different stages.

Stage	Pathway	P-value	DE genes	Upregulated	Downregulated
1 (Proliferating)	No significatively affected pathways				
2 (Fusing)	Cytokine-cytokine receptor interaction (mmu04060)	1.64E-07	23	3	20
	Focal adhesion (mmu04510)	1.48E-03	14	7	7
	Glutathione metabolism (mmu00480)	1.90E-03	7	1	6
	Cell adhesion molecules (CAMs) (mmu04514)	1.62E-02	10	1	9
	NOD-like receptor signaling pathway (mmu0462)	2.00E-02	6	1	5
	Regulation of actin cytoskeleton (mmu04810)	2.19E-02	12	3	9
	Jak-STAT signaling pathway (mmu04630)	3.92E-02	9	1	8
	Toll-like receptor signaling pathway (mmu04620)	3.97E-02	7	0	7
	Cytosolic DNA-sensing pathway (mmu04623)	5.05E-02	5	0	5
	Chemokine signaling pathway (mmu04062)	9.17E-02	9	2	7
3 (Differentiated)	Cytokine-cytokine receptor interaction (mmu04060)	1.02E-19	61	6	55
	Chemokine signaling pathway (mmu04062)	8.05E-10	38	3	35
	NOD-like receptor signaling pathway (mmu0462)	1.77E-09	21	0	21
	Toll-like receptor signaling pathway (mmu04620)	5.09E-09	26	0	26
	Cytosolic DNA-sensing pathway (mmu04623)	2.24E-06	16	0	16
	Cell adhesion molecules (CAMs) (mmu04514)	1.15E-05	27	4	23
	Jak-STAT signaling pathway (mmu04630)	2.69E-05	26	2	24
	Apoptosis (mmu04210)	5.93E-05	18	0	18
	MAPK signaling pathway (mmu04010)	2.13E-02	28	5	23
	Calcium signaling pathway (mmu04020)	0.59E-02	20	6	14

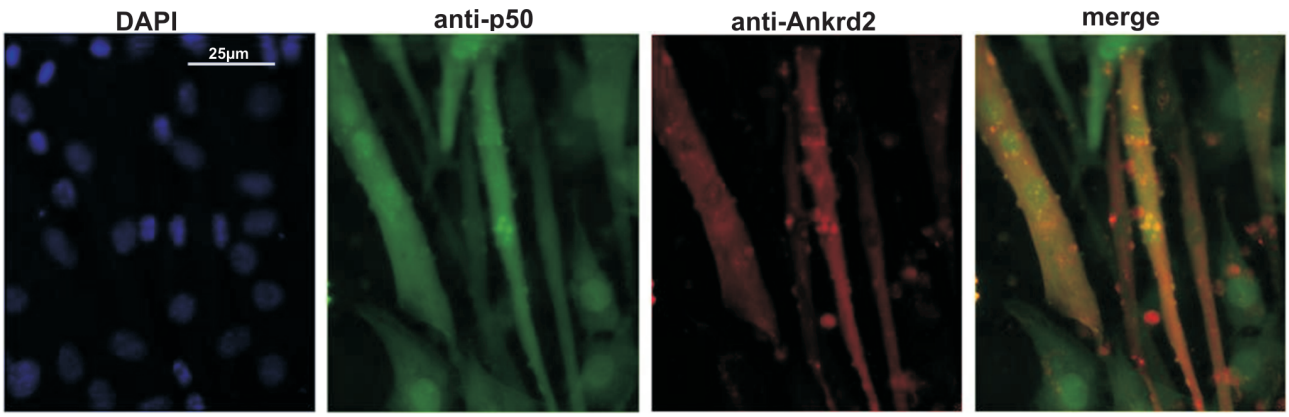

Figure S3. Exogenous Ankrd2 colocalizes with p50 in the nuclei of differentiated myotubes. C2C12 myotubes were infected with AdAnkrd2 6 days after induction of differentiation. The subcellular localization of exogenous HA-tagged Ankrd2 was detected by immunostaining with anti-HA antibody (red). Nuclei were visualized by DAPI (blue).

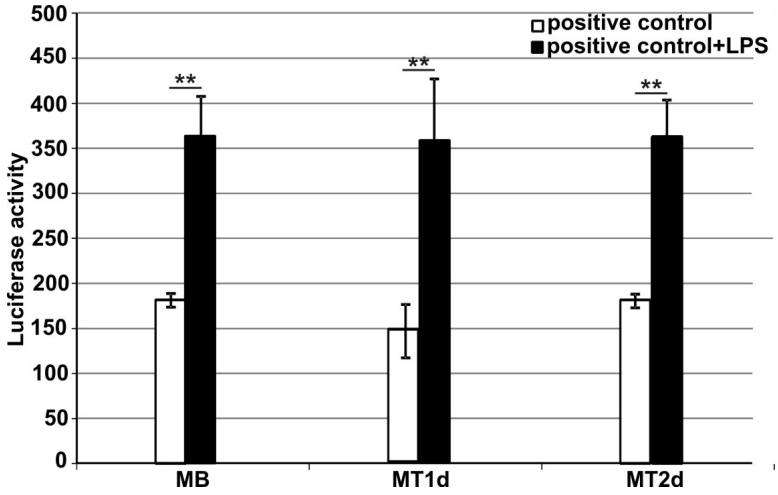

Figure S4. NF-kB activity is stimulated by bacterial lipopolysaccharides (LPS) treatment in C2C12 cells. The responsiveness to LPS treatment was determined in proliferating and differentiating C2C12 myoblasts after 1 and 2 days of induction by measurement of luciferase activity following transfection with a 3xNF-kB-luciferase vector. An about 2-fold induction in NF-kB (luciferase) activity was found in LPS-treated compared to untreated cells at all stages. All data are represented as mean±SD of three independent experiments. **P < 0.01.

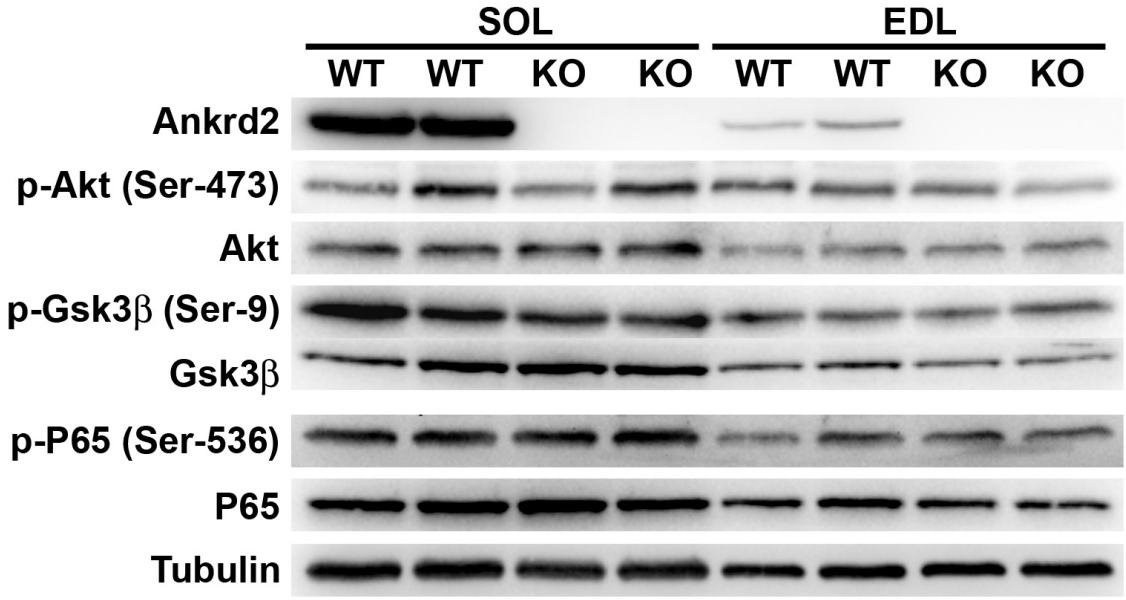

Figure S5. Ankrd2 knockout does not affect Akt, Gsk3ß, and NF-kB activity *in vivo*. Western blot analysis on soleus and EDL muscle from 3-month-old WT and Ankrd2 KO mice.

Table S2. Primer sequences for ChIP-qRT-PCR.

Name	Forward	Reverse
Proximal NF-kB box	5'-CACACTGGACAGGCCTCTTT-3'	5'-CACACTGGACAGGCCTCTTT-3'
Distal NF-kB box	5'-AGCATAGCCGTGTTTCCCTA-3'	5'-GGCTCGTTTCTCCATCTGTC-3'
Gsk3ßPRO primer0	5'-TCCTCATTGGTTATCCAGGTC-3'	5'-CTAGCCCTTCCCCACTCC-3'
Gsk3ßPRO primer1	5'-GCGGAGGACGAGTAGGAAG-3'	5'-GGCTGCTCGGGAAGTGTC-3'
Gsk3ßPRO primer2	5'-CCGAGTGACAAAGGAAGGAA-3'	5'-GAGGCAGCTCCCTTCAGAC-3'
Gsk3ßPRO primer3	5'-CGTATGGGGAGCAGTCAGG-3'	5'-AGGAGATGGCTCGGAGATG-3'
Gsk3ßPRO primer4	5'-CATCTCCGAGCCATCTCCT-3'	5'-AAGGGTGGAGTGGAATCCTT-3'
Gsk3ßPRO primer5	5'-TGAAAAGCCAAGAGAACGAA-3'	5'-CAAAAGCTGAAGGCTGCTG-3'

Table S3. Primer sequences for qRT-PCR.

Gene	Forward	Reverse
Ankrd2	5'-GAGAGCCACAGAGCTCATCG-3'	5'-GCTCTTGGCCCTTAACCTTT-3'
Ankrd1	5'-CGGACCTCAAGGTCAAGAC-3'	5'-GCTCTTCTGTTGGGAAATGC-3'
Ankrd23	5'-TGCCTAGAGCACCTTATCGAG-3'	5'-TCTGGGAAGCCACATTCTTC-3'
Il6	5'-CCACTTCACAAGTCGGAGGCTTA-3'	5'-GCAAGTGCATCATCGTTGTTCATAC-3'
Tnfα	5'- CACAAGATGCTGGGACAGTGA-3'	5'-TCCTTGATGGTGGTGCATGA-3'
IkBα	5'-GCTACTCCCCCTACCAGCTT-3'	5'-TAGGGCAGCTCATCCTCTGT-3'
Glut4	5'-TGTCGCTGGTTTCTCCAACTG-3'	5'-CCATACGATCCGCAACATACTG-3'
Rcan1	5'-GTGTGGCAAACGATGATGTC-3'	5'-AGGAACTCGGTCTTGTGCAG-3'
B2m	5'-CCGTCTACTGGGATCGAGAC-3'	5'-GCTATTTCTTTCTGCGTGCAT-3'